

Transition temperature and magnetoresistance in double-exchange compounds with moderate disorder

E. E. Narimanov¹ and C. M. Varma²¹*Electrical Engineering Department, Princeton University, Princeton, New Jersey 08544*²*Bell Laboratories—Lucent Technologies, 700 Mountain Ave., Murray Hill, New Jersey 07974*

(Received 14 February 2001; published 19 December 2001)

We develop a variational mean-field theory of the ferromagnetic transition in compounds like lanthanum-manganite within the framework of the double-exchange model supplemented by modest disorder. We obtain analytical expressions for the transition temperature, its variation with the valence electron density, and its decrease with disorder. We derive an expression for the conductivity for both the paramagnetic and the ferromagnetic metallic phases, and study its dependence on the temperature and magnetic field. A simple relation between the resistivity in the ferromagnetic phase and the spontaneous magnetization is found. Our results are in a good agreement with the experimental data on transition temperatures and resistivity in the manganite compounds with relatively small disorder. We comment on the effects of increased disorder.

DOI: 10.1103/PhysRevB.65.024429

PACS number(s): 75.30.Kz, 72.15.Gd, 75.30.Vn

I. INTRODUCTION

Interest has revived recently in the perovskite manganese oxides $A_{1-x}B_x\text{MnO}_3$ (where A is a trivalent and B is a trivalent atom), which were first investigated in the 1950s.¹ As the doping x and the temperature T are varied, these manganese oxides show a rich variety of phases.² Particularly interesting is the doping region $0.1 \leq x \leq 0.3$, where the compounds undergo a transition from either insulating or very high resistance metallic, paramagnetic phase at high temperatures to a ferromagnetic phase at low temperatures.³ Near the transition, the resistivity of the compounds changes by orders of magnitude. The application of a strong magnetic field substantially reduces this effect, thus giving rise to a very large negative magnetoresistance. The physical mechanism, responsible for this behavior, has been recently the subject of much discussion and controversy. It was initially suggested,⁴ that the colossal magnetoresistance (CMR) in manganese oxides can be explained within the framework of the double-exchange model⁵ (DE). In this model it is assumed that the on-site direct repulsion U is the largest energy, followed in order by the Hund's rule energy J and the hybridization energy t between Mn orbitals at neighboring sites. The basic conduction step is then the interchange of valence between neighboring Mn: $[\text{Mn}^{+3}\text{Mn}^{+4} \rightarrow \text{Mn}^{+4}\text{Mn}^{+3}]$. The basic physical idea of the DE mechanism is that this electron conduction is largest when the initial and the final states are degenerate. The latter requirement corresponds to an alignment of the spins of the manganese ions. In the opposite case, the conduction rate is suppressed by a factor of t/J . As a result, a transition from a paramagnetic to a ferromagnetic state leads to a dramatic increase of the conductivity of the compound. Using a dynamical mean-field calculation (DMFT),⁶ the double-exchange mechanism was successfully used^{7,8} for a quantitative description of the experimental data in LaSrMnO_3 compounds. A later study⁹ claimed that the agreement with the experiment found in Ref. 10 was caused by an unphysical choice of the density of states (DOS), and was accidental. But a calculation by Furukawa¹¹ with several different choices of the local DOS

confirmed the results of his earlier work.⁸

Subsequently a calculation carried out by the authors of Ref. 10 concluded that the double-exchange model alone could not explain the experimental data for the manganese oxides. There were two objections: (i) that the double-exchange model gave a transition temperature an order of magnitude larger than experiments and (ii) that the often observed insulatinglike resistivity (resistivity increasing with decreasing temperature) could not be explained by the double-exchange model. It was proposed in Ref. 10 that for the description of manganese oxides one should take into account a continuation to the metallic state of the Jahn-Teller distortion found for the insulating antiferromagnetic end member ($x \approx 0$) in these compounds into the x range of interest in some kind of dynamic fashion. As shown by a simple calculation,¹² objection (i) turns out to be due to an inadequate appreciation of the energetics of the double-exchange process. The transition temperature is related to the difference in the electronic cohesive energy of the ferromagnetic and paramagnetic phases, and is not given by the transition temperature of a spin model as in Ref. 10. The large change in the ionic radius of the manganese ions due to the conduction process, $\text{Mn}^{3+} \rightarrow \text{Mn}^{4+}$, does indeed lead to substantial lattice distortions. However, a substantial theoretical effort^{13,14} on the proposal of the dynamical effects of possible Jahn-Teller distortion has failed to produce any results which can be compared to experimental data for the resistivity. Nevertheless, strong electron-lattice interaction together with intrinsic disorder can lead to a static lattice disorder, which could account for insulatinglike resistivity in the manganese compounds. It was also demonstrated¹⁵ that the insulating behavior at high temperatures could be related to the interplay of lattice distortion and the effects of orbital ordering.¹⁶

Meanwhile, there has been further progress experimentally. It was only recently pointed out,¹¹ that the manganese oxides at similar electron densities show two qualitatively different types of behavior: (i) a metal-insulator transition near T_c , which in this case has relatively low values

~ 280 K, and (ii) a metallic behavior both below (a good metal) and above (incoherent metal with the absolute value of the resistivity near the Mott's limit) the critical temperature, which is comparably high (~ 380 K).¹⁷ The difference appears to be the amount of disorder. This would tend to remove the possibility that the Jahn-Teller effects, were they to occur, have much to do with the resistivity behavior. Instead the question to ask is why disorder so dramatically modifies the temperature dependence of the conductivity in the paramagnetic phase, while simultaneously reducing the transition temperature. The relation of the resistivity to the magnetization $M(T)$ in the ferromagnetic phase also depends on disorder. For small disorder the temperature dependent part is proportional to the $M(T)^2$, while for large disorder a much stronger dependence is found.

The effective strength of the intrinsic disorder is influenced by several factors, and can be characterized by the so-called ‘‘perovskite tolerance factor.’’ There is substantial empirical evidence,¹⁸ that when this number departs from the ‘‘ideal’’ value of unity, the angle between the oxygen and two neighboring manganese ions deviates from 180° , leading to microscopic inhomogeneities and to a substantial enhancement of the effective disorder. Even a small change in the perovskite tolerance factor has a substantial influence on the effective disorder in the perovskite structures, which cannot even form for the tolerance factor less than 0.9. Interestingly, the dependence of the perovskite tolerance factor on the difference in the ionic radii is not monotonic. In particular, although the ionic radius of lanthanum (1.216 \AA) is closer to the ionic radius of calcium (1.18 \AA) than to the ionic radius of strontium (1.31 \AA), for the compound $\text{La}_{0.7}\text{Sr}_{0.3}\text{MnO}_3$ the perovskite tolerance factor is closer to unity (0.93) than that of a similar structure with calcium instead of strontium (0.91). As a result, while the $\text{La}_{0.7}\text{Sr}_{0.3}\text{MnO}_3$ compound shows metallic behavior and belongs to the ‘‘weakly disordered’’ category, its calcium counterpart $\text{La}_{0.7}\text{Ca}_{0.3}\text{MnO}_3$ demonstrates metal-insulator transition and represents the ‘‘strongly-disordered’’ group.

It was suggested¹² that disorder effects due to spin-disorder, lattice polarons due to the 30% difference in the volume of the Mn^{3+} and the Mn^{4+} ions, as well as extrinsic disorder acting in concert might be responsible for the resistivity in the paramagnetic phase. The possibility suggested that spin disorder alone may be sufficient turns out, as shown by recent numerical studies, not to be correct.^{19–21} Additional randomness due to substitution disorder has been used in calculations to explain the experimental data.¹⁹ Isoelectronic $\text{La}_{0.7-x}\text{R}_x\text{Ca}_{0.3}\text{MnO}_3$ shows enormous decrease of the critical temperature²² when R is Y compared to when R is Pr. Note that the ionic radius of La^{3+} is 1.02 \AA , of Pr^{3+} is 1.01 \AA , and of Y^{3+} is 0.89 \AA . Note that the substitution with Y besides changing the average bond angle introduces disorder.

Also very interesting is the fact that not only does spin disorder disappear for $T \ll T_c$, lattice disorder does as well.^{23,24} This is evidenced by the remarkable variation of the Debye-Waller factor with temperature below and above T_c . It is clear that spin and lattice disorder act in concert and quite unusual ways. Further that quenched lattice disorder

generates extra lattice disorder which is annealed in the ferromagnetic phase.

If indeed the difference in the properties of the CMR materials is caused by the effect of the substitutional disorder, then it might be possible to account for the main features of the behavior of the ‘‘paramagnetic-metallic’’ compounds using the ‘‘pure’’ double-exchange model. To address this question is one of the main objectives of the present paper. We also consider the effect of the substitutional disorder, and show that it leads to a substantial decrease of the critical temperature of the para- to ferromagnetic transition, in agreement with the observed difference in T_c in different CMR materials. In a future paper we hope to address the more subtle issues connected with cation and other disorder in the mixed-valent compounds.

The paper is organized as follows. In the next section, we develop the variation mean-field theory for the double-exchange Hamiltonian. This is a systematization of the ansatz used in Ref. 12. We calculate the spin distribution function, and the critical temperature of the ferromagnetic transition. In the third section, we study the effect of the substitution disorder on this phase transition. In Sec. IV we develop a semiclassical transport theory for the CMR compounds, and calculate the magnetic field and temperature dependence of the resistivity. We close with a summary and discussion of future directions.

II. VARIATIONAL MEAN-FIELD THEORY

In the semiclassical limit of large spin S of the manganese ions, the effective electron Hamiltonian in the double-exchange model can be expressed as²⁵

$$H_{\text{eff}} = \frac{1}{2} \sum_{\langle ij \rangle} t_0 \cos(\theta_{ij}/2) c_i^\dagger c_j + \sum_i [v_i c_i^\dagger c_i - \mu_B S B \cos \vartheta_i], \quad (1)$$

where the first sum includes hopping only between the nearest-neighbor manganese ions of different valencies, the angle θ_{ij} is defined as the angle between the ion spins \mathbf{S}_i and \mathbf{S}_j , v_i represents the effect of the substitutional disorder, B is the magnetic field, and μ_B is the Bohr magneton. The angle ϑ is the angle between the spin \mathbf{S}_i and the magnetic field. It is important to note that the assumption of large U and J compared to t makes the charge carriers effectively spinless.

Neglecting the correlations in the orientations of the neighbor spins, we represent the free energy F of the system in terms of the single spin orientation distribution function $P_\Omega(\boldsymbol{\Omega})$. In the mean-field approximation, the distribution function depends only on the angle ϑ between the local spin and the external magnetic field B :

$$P_\Omega = \frac{1}{2\pi} P_\vartheta(\vartheta). \quad (2)$$

In the semiclassical limit, the corresponding spin entropy is then

$$S_{\text{spins}} = - \int d\vartheta \sin \vartheta P_\vartheta(\vartheta) \ln [P_\vartheta(\vartheta)] + S_{\text{spins}}^0(S), \quad (3)$$

where the function $S_{\text{spins}}^0(S)$ does not depend on P_{ϑ} , and is related to our choice of the normalization of the spin distribution function $\int d(\cos \vartheta) P_{\vartheta}=1$. This semiclassical approximation is discussed in detail in Appendix A.

The calculation of the energy for a given spin distribution is more complicated. When the transfer integral between the neighboring sites i and j is equal to a constant value \tilde{t} , and the effects of the substitution disorder can be ignored, the electron energy is given by

$$E_t[\tilde{t}] = \int_{-\infty}^{\mu} d\varepsilon \rho_0(\tilde{t}; \varepsilon) \varepsilon, \quad (4)$$

where ρ is the electron density of states (DOS) corresponding to the Hamiltonian (1) with no diagonal disorder ($v_i=0$) and constant transfer integral $t_{ij}=t$. To account for the effects of the substitution disorder v_i , we introduce an effective averaged DOS defined as

$$\rho(t, \varepsilon) = \langle \rho_0(t, \varepsilon - v) \rangle_v, \quad (5)$$

where the average is performed over the distribution of the v_i 's.

To obtain the total energy, in the mean-field approximation we average $E_t[\tilde{t}]$ over the distribution of the transfer integrals,

$$E = \int dt P_t(t) E_t[\tilde{t}]. \quad (6)$$

The transfer integral t_{ij} can then be expressed in terms of the polar angles (ϕ_i, ϑ_i) and (ϕ_j, ϑ_j) , which define the orientations of the corresponding spins, since they uniquely define the relative angle θ . Therefore the integration over t in Eq. (6) can be converted to the integration over the polar angles. Using the procedure discussed in detail in Appendix B, we derive the effective free-energy functional, and by a direct minimization obtain the following integral equation for the spin distribution function:

$$\begin{aligned} P_{\vartheta}(\vartheta) = & \exp \left[-2 \int_0^{2\pi} \frac{d\phi_1}{2\pi} \int_0^{2\pi} \frac{d\phi_2}{2\pi} \int_0^{\pi} d\vartheta_1 \sin \vartheta_1 P_{\vartheta}(\vartheta_1) \right. \\ & \times \int_{-\infty}^{\mu} d\varepsilon \frac{\varepsilon - \mu}{T} \rho \left(t_0 \cos \left(\frac{\theta}{2} \right); \varepsilon \right) \\ & \left. - \frac{\zeta}{T} + \frac{\mu_B S B}{T} \cos \vartheta \right]. \end{aligned} \quad (7)$$

Here the parameter $\zeta = \zeta(T, B)$ accounts for the proper normalization of the distribution function P_{ϑ} . The last term accounts for the energy $\mu_B S B \cos \vartheta$ of the spin, tilted at the angle ϑ with respect to the direction of the external magnetic field. Finally, the first term in the exponential of Eq. (7) represents the energy of the electron gas, which depends on the spin distribution via the effective ‘‘local’’ bandwidth $W \sim \cos \theta/2$, determined by the relative orientation of the near spins. Note that this term depends nontrivially on ϑ via the relative angle $\theta = \theta(\phi_1, \vartheta_1; \phi, \vartheta)$. This nonlinear integral equation allows a straightforward numerical solution by it-

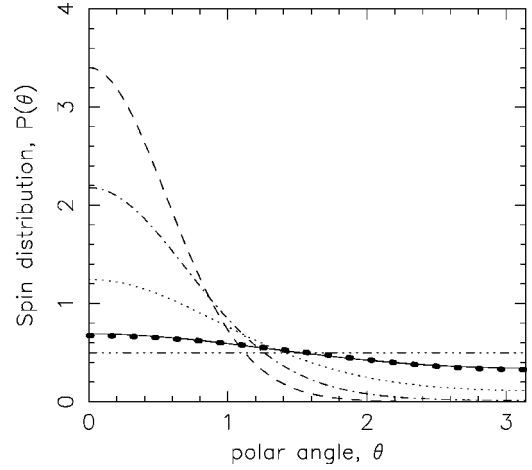


FIG. 1. The distribution P_{ϑ} , for $T/T_c=0.5$ (dashed line), 0.7 (dashed-dotted line), 0.9 (dotted line), 0.99 (solid line), 1.01 (dashed-triple-dotted line). The line of large dots represents the ‘‘linear’’ approximation of Eq. (9), appropriate for a small magnetization.

erations. In Fig. 1 we plot the distribution P_{ϑ} for different values of the scaled temperature $\tau \equiv T/t_0$ and dimensionless magnetic field $b \equiv B/t_0$.

When the magnetization of the system is small, and the spin distribution is close to uniform (e.g., when the system is in the paramagnetic phase in a small external field), then the distribution function

$$P_{\vartheta}(\vartheta) = \frac{1}{2} + \delta p_{\vartheta}(\vartheta), \quad \delta p_{\vartheta} \ll 1. \quad (8)$$

Expanding the exponential in the right-hand side of Eq. (7) in δp_{ϑ} , and keeping the terms up to the first order in δp_{ϑ} , yields

$$\delta p_{\vartheta} = \frac{3}{2} M(T, B) \cos \vartheta + \mathcal{O}(M^2), \quad (9)$$

where $M(T, B) = \chi(T)B + \mathcal{O}(B^2)$ is the magnetization of the system. The susceptibility χ is then given by

$$\chi(T) = \frac{1}{3} \frac{\mu_B^2 S^2}{T - T_c}, \quad (10)$$

where the critical temperature T_c is given by

$$T_c = \int_0^{\pi} d\vartheta \sin \vartheta \cos \vartheta \int_{-\infty}^{\mu} d\varepsilon (\mu - \varepsilon) \rho \left(t_0 \cos \frac{\vartheta}{2}; \varepsilon \right). \quad (11)$$

For a system without intrinsic disorder, Eq. (11) yields the values of the critical temperature consistent with the results obtain using other methods.^{4,11,26–29} For example, for $x=0.25$ we obtained $T_c/W \approx 0.016$, while a high-temperature series expansion²⁶ yields $T_c/W \approx 0.013$, the Monte Carlo calculation²⁷ yields $T_c/W \approx 0.0125$, the method of Ref. 28 yields $T_c/W \approx 0.066$, and different numerical calculations within the framework of dynamical mean-field theory yield

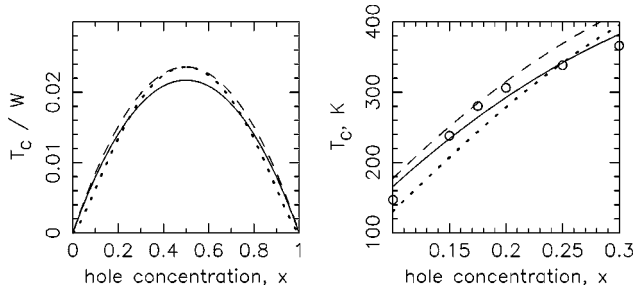


FIG. 2. The dependence of the critical temperature on the electron concentration. The dotted and solid lines correspond to, respectively, rectangular and Gaussian DOS. The dashed line represents the $x(1-x)$ dependence obtained in Ref. 12. The circles are the experimental data of Ref. 8. The left panel shows T_c in units of bandwidth W , while the absolute units for the right panel were calculated, assuming $W=1.8$ eV.

$T_c/W \approx 0.043$ (Ref. 9) and $T_c/W \approx 0.046$.²⁹ As all these calculations are either of the mean-field type or involve a numerically exact calculation of only a small cluster of sites, the difference in the results by a factor of 3 is not surprising.

It is also worth noting that the relation of this theory to the approach developed in Ref. 12. There, in addition to the mean-field approximation, a specific functional form of the probability distribution of the angle between different spins was assumed, with the system magnetization being the variational parameter. This should be contrasted to the method of the present paper, when the functional form of the single-spin distribution function is derived variationally. The general dependence of the distribution derived here turns out to be quite similar to the one assumed earlier. But the results of the variational procedure developed in this section should be more accurate besides being on firmer ground. Another advantage of the present method is that it can be used for the description of the effects of the substitution disorder—something which is hard to characterize within the framework of Ref. 12.

As follows from Eq. (11), the critical temperature explicitly depends on the density of states, and the resulting value is in fact sensitive to the actual shape of DOS. However, this has only a marginal effect on the dependence of T_c on the concentration x . To illustrate this behavior, in Fig. 2 we plot the critical temperature as a function of the charge carrier concentration x for a rectangular (blue curve) and Gaussian (red curve) densities of states. For comparison, we also plot the $x(1-x)$ dependence (black line), obtained in an earlier work,¹² and the experimental data of Ref. 10. The model densities of states are plotted in Fig. 3 and compared to the DOS ρ_t , corresponding to the Hamiltonian (1) with constant transfer integral and no diagonal disorder. The effective bandwidth of the model densities of states is chosen to accurately reproduce the second moment $\langle \varepsilon^2 \rangle$. Note how accurately the Gaussian density of states fits the profile of ρ_t .

As follows from Fig. 2, a reasonable choice of the bandwidth $W=1.8$ eV, consistent with the calculations in the local-density approximation,³⁰ leads to a good agreement with the experimental data. One has, however, to keep in mind that the estimates for the bandwidth in the literature

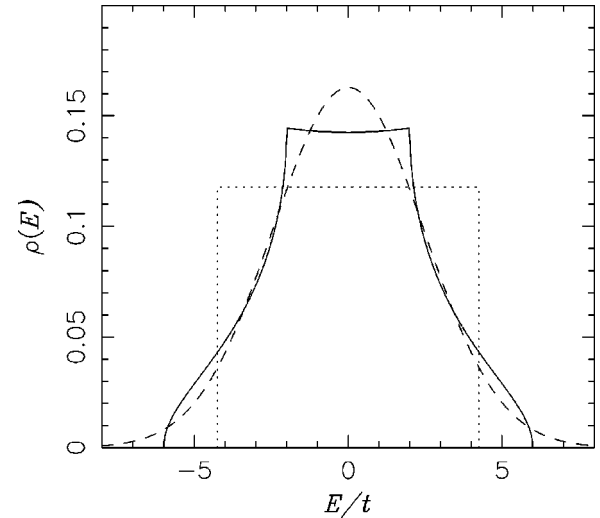


FIG. 3. The model rectangular (dotted line) and Gaussian (dashed line) densities of states, and the actual DOS $\rho_t(\varepsilon)$ (solid line). For each model density of states, the bandwidth is chosen such that the second moment $\langle \varepsilon^2 \rangle$ is exact. Note how accurately the Gaussian DOS fits the profile of ρ_t .

differ substantially and range from ~ 1 eV (Ref. 31) to ~ 4 eV,^{32,33} which, e.g., for $x=0.3$ will correspond for the variation of the critical temperature from 210 to 840 K. One should, however, keep in mind that the main objective of the variational mean-field theory developed in the present paper is not a quantitative calculation of the critical temperature for some given composition, but to describe the variation of T_c with the carrier concentration and effective disorder, and to uncover the physical origin of this behavior.

As explained earlier,¹² the transition temperature is determined essentially by the difference in the cohesive energy of the ferromagnet and the paramagnet by the entropy of the paramagnet. The larger bandwidth of the ferromagnet by about 20% is the essential aspect of the energetics in the double-exchange problem.

Consider now the effect of substitutional disorder. Substitutional disorder increases the electron-bandwidth for the paramagnet. The removal of spin-disorder is then expected to decrease the change in the bandwidth on becoming a ferromagnet. This is explicitly borne out by the theory here.

Since the critical temperature is directly related to the effective DOS, it is sensitive to the substitution disorder in the system. Assuming the Gaussian distribution of the disorder strength v_i with the standard deviation V_0 and Gaussian “bare” DOS (Ref. 34) $\rho_g \propto \exp[-\varepsilon^2/(3t^2)]$, we obtain

$$T_c = \int_0^\pi d\vartheta \int_{-\infty}^\mu d\varepsilon (\mu - \varepsilon) \rho[t_{\text{eff}}(\vartheta), \varepsilon] \sin \vartheta \cos \vartheta, \quad (12)$$

where the effective transfer integral t_{eff} is defined by the equation

$$\frac{1}{t_{\text{eff}}^2} = \frac{1}{t_0^2 \cos^2 \frac{\vartheta}{2}} + \frac{3}{V_0^2}. \quad (13)$$

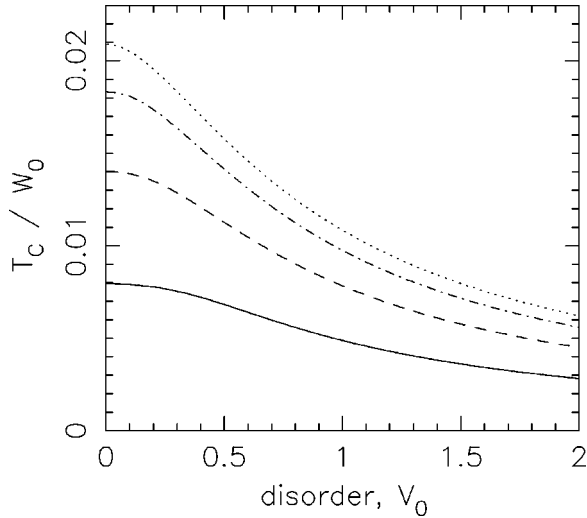


FIG. 4. The dependence of the critical temperature on the average “disorder” v_0 (in units of the bandwidth W_0 of the “clean” system $v=0$). Curves of different styles represent different electron concentrations (from top to bottom: $x=0.4, 0.3, 0.2, 0.1$). The distribution of the disorder energies v_i is Gaussian.

The dependence (12) is shown in Fig. 4 for different electron concentrations. As extra disorder makes the ferromagnetic phase less favorable, the critical temperature goes down with an increase of V_0 .

It might be tempting to attribute the difference in critical temperature between the “type-I” and “type-II” compounds to the effect of the substitutional disorder. In such model, an effective disorder strength of $V_0 \sim 0.7W$ would fully account for only $\sim 30\%$ difference in the critical temperatures of type-I and type-II compounds. We suspect that large enough lattice disorder in concert with lattice disorder localizes electronic states in the paramagnetic phase. New considerations then enter in to the determination of the transition temperature. These will be discussed separately. Also missing from the discussion above is the effect of the formation of spin polarons which must occur in the paramagnetic phase.^{12,35} They would tend to decrease T_c but the number of spins in the polarons is rather small and only a modest numerical effect on the transition temperature is expected. They are, however, quite important for the dynamics near the transition.

III. RESISTIVITY WITHOUT LATTICE DISORDER: SEMICLASSICAL TREATMENT

In the mean-field approximation developed in the previous section, each spin independently fluctuates around the

averaged value defined by the magnetization of the system. From the point of view of the semiclassical transport theory, that would correspond to effective independent “scatterers” located at each point of the lattice. However, in the ferromagnetic phase, when the spin fluctuations are small compared to the averaged value, the corresponding electron mean free path may be substantially larger than the (Mn) lattice spacing. In this limit, in order to estimate the resistivity of the system, we can use the standard semiclassical transport theory.

We introduce the average transfer integral $\bar{t} \equiv t_0 \langle \cos(\theta_{\alpha\beta}/2) \rangle$, so that the corresponding unperturbed Hamiltonian is defined as

$$H_0 = \frac{1}{2} \sum_{\langle \alpha\beta \rangle} \bar{t} c_{\alpha}^{\dagger} c_{\beta} \quad (14)$$

and the rest of H is treated as the “perturbation,”

$$V = \frac{1}{2} \sum_{\langle ij \rangle} \delta t_{ij} c_i^{\dagger} c_j. \quad (15)$$

The standard plane-wave diagonalization of H_0 yields the dispersion law

$$\epsilon_{\mathbf{k}} = \bar{t} [\cos(k_x a) + \cos(k_y a) + \cos(k_z a)] \quad (16)$$

which describes “holes” near $\mathbf{k}=0$ and “electrons” near, e.g., $\mathbf{k} = \pi/a(1,1,1)$. When the Fermi energy is located near the bottom or near the top of the band, one can define the effective mass for the electrons and the holes, respectively, $m_* = 2\bar{t}a^2/\hbar^2$.

The kinetic equation for the electron distribution function $f_{\mathbf{k}}$ is³⁶

$$-e\mathbf{E} \frac{\partial f^0}{\partial \mathbf{k}} = \frac{2\pi}{\hbar} \sum_{\mathbf{k}'} |\langle \mathbf{k} | V | \mathbf{k}' \rangle|^2 \delta(\epsilon_{\mathbf{k}} - \epsilon_{\mathbf{k}'}) (f_{\mathbf{k}} - f_{\mathbf{k}'}), \quad (17)$$

where $f^0(\epsilon_{\mathbf{k}})$ is the equilibrium distribution function, and $\langle \mathbf{k} | V | \mathbf{k}' \rangle$ is the matrix element of the “perturbation” (15).

The kinetic equation (17) has the solution

$$f_{\mathbf{k}} = f^0(\epsilon_{\mathbf{k}}) - eE\tau(\mathbf{k}) \frac{\partial \epsilon_{\mathbf{k}}}{\partial k_z} \frac{\partial f^0(\epsilon_{\mathbf{k}})}{\partial \epsilon_{\mathbf{k}}}, \quad (18)$$

where the relaxation time is defined by the following equation:

$$\frac{1}{\tau(\mathbf{k})} = \frac{3a^3}{2\pi^2\hbar} \overline{\delta t^2} \int d\mathbf{k}' \left(1 + \frac{\epsilon_{\mathbf{k}+\mathbf{k}'}}{6\bar{t}} \right) \delta(\epsilon_{\mathbf{k}} - \epsilon_{\mathbf{k}'}) - \frac{a^3}{2\pi^2\hbar} \overline{\delta t^2} \int d\mathbf{k}' \sin^2(k'_z a) \delta(\epsilon_{\mathbf{k}} - \epsilon_{\mathbf{k}'}). \quad (19)$$

Assuming a *uniform* dispersion $\epsilon_{\mathbf{k}} = \epsilon(|\mathbf{k}|)$, this expression reduces to the standard result for the transport relaxation time,

$$\frac{1}{\tau(k)} = \int d\mathbf{k}' W_{\mathbf{k}\mathbf{k}'} (1 - \cos \theta_{\mathbf{k}\mathbf{k}'}) \delta(\epsilon_{\mathbf{k}} - \epsilon_{\mathbf{k}'}), \quad (20)$$

where the scattering rate $W_{\mathbf{k}\mathbf{k}'} = 3a^3(2\pi^2\hbar)^{-1}\overline{\delta t^2}[1 + \epsilon_{\mathbf{k}+\mathbf{k}'}/(6\bar{t})]$, and $\theta_{\mathbf{k}\mathbf{k}'}$ is the angle between the vectors \mathbf{k} and \mathbf{k}' .

Near the top and the bottom of the band, the integrals in Eq. (19) allow a straightforward analytical evaluation. For example, for the holes we obtain

$$\tau^{-1}(\mathbf{k}) = \frac{6}{\pi\hbar} ka \left(1 - \frac{2}{9}(ka)^2 \right) \frac{\overline{\delta t^2}}{\bar{t}}. \quad (21)$$

As we pointed out before, the semiclassical approach developed in the present section is appropriate only when the charge-carrier mean free path $\ell \gg a$. Using Eq. (21) for the ratio of the mean free path to the lattice spacing near the top of the band we obtain

$$\frac{\ell}{a} = \frac{\bar{t}^2}{\overline{\delta t^2}} \frac{3}{\pi \left[1 - \frac{2}{9}(ka)^2 \right]}. \quad (22)$$

As follows from Eqs. (19) and (22), in the absence of substitution disorder, ℓ/a is *always* greater than $(3/\pi) * (\bar{t}^2/\overline{\delta t^2})$. The ratio $\bar{t}^2/\overline{\delta t^2}$ is a monotonically decreasing function of temperature in the ferromagnetic phase, and constant above the T_c , where $\bar{t}^2/\overline{\delta t^2} = 8$. Therefore, since the mean free path due to the spin disorder is substantially larger than the effective lattice spacing, we expect that in the relevant concentration range $x \approx 0.1-0.3$ such a ‘‘pure DE’’ system would generally show the metallic behavior. Indeed, in a typical type-II compound $\text{La}_{0.7}\text{Sr}_{0.3}\text{MnO}_3$, the resistivity does show the metallic behavior $d\rho/dT > 0$ both above and below the transition.⁸

The effect of nonzero magnetization (caused either by the transition to the ferromagnetic phase, or by external magnetic field) on the conductivity is twofold: first, it suppresses the fluctuations in transfer integrals thus decreasing the corresponding scattering rate; second, the increase of the *average* transfer integral caused by the magnetization leads to a decrease of the effective mass $m_* \sim 1/\bar{t}$. Both these factors lead to a decrease of the resistivity ρ . For a small magnetization,

$$\rho(M) = \rho_0 [1 - \kappa(M/M_{\max})^2], \quad (23)$$

where in the effective-mass approximation the coefficient κ is equal to $9/5$. For weakly disordered manganites, the resistivity indeed follows Eq. (23). As seen in the inset in Fig. 5(b) the experimental value is about 2 and slowly varies with the electron density. Taking into account the band nonparabolicity leads to a weak dependence of κ on the concentration x , but does not fully account for an increase of κ . The variation of the resistivity in the whole range of the sample magnetization $0 < M < M_{\max}$ is shown in Fig. 5.

Using the semiclassical approach developed in the present section, one can also obtain an analytic expression for the

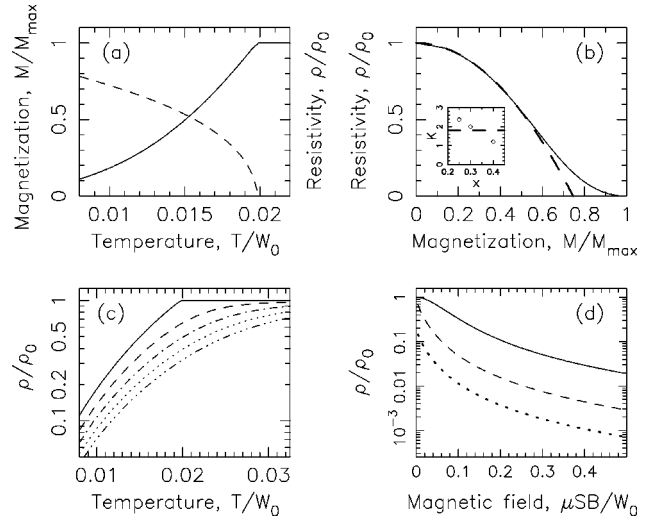


FIG. 5. The resistivity and magnetization of the sample, calculated using in the variational mean-field approximation for the DE model. (a) The variation of the resistivity (solid line) and magnetization (dashed line) with temperature, in the absence of external magnetic field. (b) The resistivity as a function of magnetization, the inset shows the variation of the coefficient κ with concentration x , obtained from the experimental data (Ref. 37), and the theoretical prediction in the effective-mass approximation (dashed line). (c) The resistivity as a function of temperature, for different values of the magnetic field. From top to bottom, solid line: $\mu SB/W_0 = 0$; dashed line: $\mu SB/W_0 = 0.005$; dashed-dotted line: $\mu SB/W_0 = 0.01$; dotted line: $\mu SB/W_0 = 0.015$; dashed-triple-dotted line: $\mu SB/W_0 = 0.02$. (d) The resistivity as a function of magnetic field, for different temperatures. From top to bottom, solid line: $T/W_0 = 0.05$; dashed line: $T/W_0 = 0.02$; dotted line: $T/W_0 = 0.01$.

zero-field resistivity ρ_0 . However, the behavior above the critical temperature is characterized by the formation of small magnetic polarons, localized due to the spin disorder.¹² In a nonzero magnetic field, this effect also affects the magnetization and is taken into account phenomenologically by using the actual experimentally observed magnetization M in Eq. (23). However, the present Boltzmann-type approach is not adequate for a quantitative calculation of the zero-field resistivity ρ_0 .

The quadratic dependence of the resistivity on the magnetization in manganites was also obtained in Refs. 6 and 38. The prefactor we obtain in the present work is similar to the one calculated by Furukawa in Ref. 6, and agrees with the experiment better than the result of Inoue and Maekawa.³⁸ However, as all three methods are essentially mean-field theories with a number of nontrivial approximations, the marginal difference obtained for the prefactor is not very important. Instead, the advantage of the approach presented in this paper is that it makes much more transparent the physics underlying the behavior of colossal magnetoresistance compounds—which is much harder to achieve using, e.g., the numerical dynamical mean-field theory used earlier.

IV. SUBSTITUTION DISORDER: EFFECT ON RESISTIVITY

As we pointed out in Sec. II, the 30% difference in the critical temperatures of the type-I and type-II compounds

implies that in the “disordered” compounds the effective scattering potential is of the order of the electron bandwidth. In such conditions, the localization effects can become important, and the semiclassical treatment of the previous section is no longer appropriate.

It has been proposed that in the “strongly disordered” (type-I) compounds, the ferro- to paramagnetic phase transition drives the metal-insulator transition. In the paramagnetic phase, the “combined effort” of the substitution and spin disorder is sufficient to localize the charge carriers, while in the ferromagnetic phase, due to larger electron bandwidth and weaker spin disorder, the mobility edge is below the Fermi energy.^{12,22}

One might be tempted to think that this mechanism of the colossal magnetoresistance of the disordered manganites reduces the problem to an Anderson-type transition as a function of disorder alone, where the spin disorder is a function of the magnetization. This is not correct since the magnetic entropy is essential to the transition which occurs at a finite temperature unlike the Anderson transition which occurs at $T=0$.

An important question, however, is whether the resistivity near the transition can be expressed uniquely as a function of magnetization. If the phase transition (with or without “diagonal” disorder) is characterized by a divergent magnetic correlation length scale, this may be possible. It should be remembered, however, that resistivity depends on fluctuations at large momentum transfer. In a solid with lattice disorder, the ferromagnetic correlation length does not uniquely characterize the important disorder at short length scales even though it may be coupled to the magnetization as appears to be the case in the manganites. It is also possible that for sufficiently strong disorder, the ferromagnetic transition is replaced by a crossover and there is no divergent correlation length. These are probably the reasons why no clear indication of scaling behavior expected in a continuous quantum phase transition were found in the recent resistivity measurements.^{39,40} These considerations, however, go beyond the mean-field-type theory developed in the present paper.

In any case, we believe that in order to fully understand the physics underlying the colossal magnetoresistance in doped manganites, one also has to take into account the lattice disorder, which is coupled to the spin disorder, via their influence on the charge carriers. Indeed, the strong coupling between the spin and lattice disorder was recently demonstrated in two independent experiments.^{24,25} Clearly, the effective lattice disorder has its own nontrivial temperature dependence, and, being coupled to the charge carriers, therefore obviously leads to substantial deviations from the standard picture of the “static” Anderson metal-insulator transition. However, at this point we defer the further description of this effect.

V. CONCLUSIONS

As shown in the first part of the present paper, the phase transition from paramagnetic to ferromagnetic phase in relatively pure manganese oxides can be successfully described

by a variational approximation on the double-exchange Hamiltonian. The results obtained for the critical temperature and its evolution with doping and the chemical composition of the compound are consistent with the experimental data. The decrease of T_c with modest disorder is also understood.

The resistivity of the type-II manganese compounds can also be successfully described using the DE model. We showed that, e.g., the theoretical dependence of the resistivity on the sample magnetization is in a quantitative agreement with the experimental data. Our calculations show the robustness of the results to the particular choice of the electron density of states, as should be obvious since the transition temperature depends on the difference of the cohesive energy of the paramagnetic and the ferromagnetic phases.

The principal problems of the manganites left unanswered in this paper concern the properties of the type-I compounds and the remarkable effects of disorder in them in both the dynamic and static properties. These are also the more subtle problems. Especially interesting is the fact that extrinsic disorder appears to promote some additional disorder in the paramagnetic phase which is swept away together with the spin disorder in the ferromagnetic phase. We hope to provide an answer to these questions separately.

APPENDIX A: SPIN ENTROPY IN THE SEMICLASSICAL MEAN-FIELD APPROXIMATION

In the mean-field approximation, when the spin-density matrix of the whole system $\rho^\Sigma(S_z^{(i)})$ is represented as a product of diagonal density matrices $\rho_i = \rho^{(1)}(S_z^{(i)})$ of the individual spins,

$$\rho^\Sigma = \prod_{i=1}^N \rho_i. \quad (\text{A1})$$

Then the total spin entropy

$$S_{\text{spins}}^\Sigma = \text{Tr}\{\rho^\Sigma \ln[\rho^\Sigma]\} \quad (\text{A2})$$

is represented by

$$S_{\text{spins}} = N \sum_{S_z=-S}^S \rho^{(1)}(S_z) \ln[\rho^{(1)}(S_z)]. \quad (\text{A3})$$

In the semiclassical approximation $S \gg 1$, the summation over S_z can be replaced by integration. Introducing the new variable $\vartheta \equiv \arccos(S_z/S)$, we obtain

$$S_{\text{spins}} = NS \int_{-1}^1 d \cos \vartheta \rho^{(1)}(S \cos \vartheta) \ln[\rho^{(1)}(S \cos \vartheta)], \quad (\text{A4})$$

where $\rho^{(1)}(S \cos \vartheta)$ is normalized as follows:

$$1 = \sum_{S_z=-S}^S \rho^{(1)}(S_z) = S \int_{-1}^1 d \cos \vartheta \rho^{(1)}(S \cos \vartheta). \quad (\text{A5})$$

We now define the spin orientation distribution function $P_\vartheta \sim \rho^{(1)}(S \cos \vartheta)$, normalized as

$$\int_{-1}^1 d \cos \vartheta \rho^{(1)}(S \cos \vartheta) = 1. \quad (\text{A6})$$

As follows from Eqs. (A5) and (A6), the spin orientation distribution function

$$P_{\vartheta} = \frac{1}{S} \rho^{(1)}(S \cos \vartheta). \quad (\text{A7})$$

Therefore the semiclassical spin entropy

$$S_{\text{spins}} = -N \int_{-1}^1 d \cos \vartheta P_{\vartheta} \ln[P_{\vartheta}] + N \ln[S]. \quad (\text{A8})$$

For example, in the paramagnetic phase, when there are no external fields, and the spin orientation distribution is uniform, $P_{\vartheta} = 1/2$, the semiclassical spin entropy is equal to $N \ln(2S)$, which is consistent with the exact result $N \ln(2S + 1)$ for $S \gg 1$. Note that the main contribution to the semiclassical spin entropy comes actually from the distribution-independent term in Eq. (A8).

The semiclassical description, however, fails for large magnetization, when the spin system is almost completely polarized, and the distribution function starts to change substantially on the scale of $\delta\vartheta \sim 1/S$. In this case, the original expression, Eq. (A3), should be used for the calculation of the spin entropy.

APPENDIX B: VARIATIONAL FREE-ENERGY FUNCTIONAL

In this appendix, we calculate the variational free-energy functional for the double-exchange model. Using Eqs. (4) and (6), for the electron energy we obtain

$$\begin{aligned} E_e &= \int_0^{2\pi} \frac{d\phi_1}{2\pi} \int_0^{2\pi} \frac{d\phi_2}{2\pi} \int_0^{\pi} d\vartheta_1 \sin \vartheta_1 \\ &\times \int_0^{\pi} d\vartheta_2 \sin \vartheta_2 P_{\vartheta}(\vartheta_1) P_{\vartheta}(\vartheta_2) \\ &\times \int_{-\infty}^{\mu} d\varepsilon \varepsilon \rho \left(t_0 \cos \left(\frac{\theta(\phi_1, \vartheta_1; \phi_2, \vartheta_2)}{2} \right); \varepsilon \right) \end{aligned} \quad (\text{B1})$$

while the extra spin energy

$$E_s = -B \int_0^{2\pi} \frac{d\phi_1}{2\pi} \int_0^{\pi} d\vartheta_1 \sin \vartheta_1 \cos \vartheta_1 P_{\vartheta}(\vartheta_1). \quad (\text{B2})$$

The free energy can be obtained by the substituting these expressions and the entropy (3) into the standard definition of the free energy

$$F = E_e + E_s - TS. \quad (\text{B3})$$

In order to find the single-spin distribution P_{ϑ} , one has to minimize the effective free energy, taking into account the constraints of normalization. Using the standard Lagrange multiplier method, for the effective free-energy functional we obtain

$$\begin{aligned} \bar{F}[P_{\vartheta}; \mu, \lambda, \zeta] &= \int_0^{2\pi} \frac{d\phi_1}{2\pi} \int_0^{2\pi} \frac{d\phi_2}{2\pi} \int_0^{\pi} d\vartheta_1 \sin \vartheta_1 \\ &\times \int_0^{\pi} d\vartheta_2 \sin \vartheta_2 P_{\vartheta}(\vartheta_1) P_{\vartheta}(\vartheta_2) \\ &\times \int_{-\infty}^{\mu} d\varepsilon (\varepsilon - \lambda) \rho \left(t_0 \cos \left(\frac{\theta}{2} \right); \varepsilon \right) \\ &+ T \int_0^{2\pi} \frac{d\phi_1}{2\pi} \\ &\times \int_0^{\pi} d\vartheta_1 \sin \vartheta_1 P_{\vartheta}(\vartheta_1) \ln[P_{\vartheta}(\vartheta_1)] \\ &- B \int_0^{2\pi} \frac{d\phi_1}{2\pi} \int_0^{\pi} d\vartheta_1 \sin \vartheta_1 \cos \vartheta_1 P_{\vartheta}(\vartheta_1) \\ &+ \zeta \int_0^{\pi} d\vartheta \sin \vartheta p_{\vartheta}(\vartheta) + \bar{F}[x, \lambda, \zeta], \end{aligned} \quad (\text{B4})$$

where the ‘‘constant’’ \bar{F} represents the spin distribution-independent part of the free energy. Here, the Lagrange multiplier ζ accounts for the normalization of the distribution function P_{ϑ} , while the Lagrange multiplier λ represents the constraint of having a fixed concentration of mobile electrons in the system.

It is straightforward to show by a direct calculation that at the extremum of the functional (B4) $\lambda = \mu$. This has a clear physical meaning—the Lagrange multiplier λ corresponds to the electron number conservation, and therefore should be equal to the electron electrochemical potential. Replacing λ by μ in Eq. (B4), we finally obtain the effective mean-field-free energy functional:

$$\begin{aligned} \bar{F}[P_{\vartheta}; \mu, \lambda, \zeta] &= \int_0^{2\pi} \frac{d\phi_1}{2\pi} \int_0^{2\pi} \frac{d\phi_2}{2\pi} \int_0^{\pi} d\vartheta_1 \sin \vartheta_1 \\ &\times \int_0^{\pi} d\vartheta_2 \sin \vartheta_2 P_{\vartheta}(\vartheta_1) P_{\vartheta}(\vartheta_2) \\ &\times \int_{-\infty}^{\mu} d\varepsilon (\varepsilon - \mu) \rho \left(t_0 \cos \left(\frac{\theta}{2} \right); \varepsilon \right) \\ &+ T \int_0^{2\pi} \frac{d\phi_1}{2\pi} \int_0^{\pi} d\vartheta_1 \sin \vartheta_1 P_{\vartheta}(\vartheta_1) \\ &\times \ln[P_{\vartheta}(\vartheta_1)] - B \\ &\times \int_0^{2\pi} \frac{d\phi_1}{2\pi} \int_0^{\pi} d\vartheta_1 \sin \vartheta_1 \cos \vartheta_1 P_{\vartheta}(\vartheta_1) \\ &+ \zeta \int_0^{\pi} d\vartheta \sin \vartheta p_{\vartheta}(\vartheta) + \bar{F}. \end{aligned} \quad (\text{B5})$$

Taking the functional derivative of Eq. (B5) with respect to P_{ϑ} , for the distribution we obtain

$$P_{\vartheta}(\vartheta) = \exp \left[-2 \int_0^{2\pi} \frac{d\phi_1}{2\pi} \int_0^{2\pi} \frac{d\phi_2}{2\pi} \int_0^{\pi} d\vartheta_1 \sin \vartheta_1 P_{\vartheta}(\vartheta_1) \int_{-\infty}^{\mu} d\varepsilon \frac{\varepsilon - \mu}{T} \rho \left(t_0 \cos \left(\frac{\theta}{2} \right); \varepsilon \right) - \frac{\zeta}{T} + \frac{B}{T} \cos \vartheta \right]. \quad (\text{B6})$$

Note that the exponential on the right-hand side nontrivially depends on ϑ via the angle $\theta = \theta(\phi_1, \vartheta_1; \phi, \vartheta)$.

- ¹G. H. Jonker and J. H. van Santen, *Physica (Utrecht)* **16**, 337 (1950); **19**, 120 (1953).
- ²A. P. Ramirez, *J. Phys.: Condens. Matter* **9**, 8171 (1997).
- ³S. Jin, T. H. Tiefel, M. McCormack, R. A. Ramesh, and L. H. Chen, *Science* **264**, 413 (1994); M. I. Imada, A. Fujimori, and Y. Tokura, *Rev. Mod. Phys.* **70**, 1039 (1998), and references therein.
- ⁴N. Furukawa, *J. Phys. Soc. Jpn.* **63**, 3214 (1994).
- ⁵C. Zener, *Phys. Rev.* **82**, 403 (1951).
- ⁶A. Georges, G. Kotliar, W. Krauth, and M. J. Rozenberg, *Rev. Mod. Phys.* **68**, 13 (1996).
- ⁷P. G. de Gennes, *Phys. Rev.* **118**, 141 (1960).
- ⁸Y. Tokura, A. Urushibara, Y. Moritomo, T. Arima, A. Asamitsu, G. Kido, and N. Furukawa, *J. Phys. Soc. Jpn.* **63**, 3931 (1994).
- ⁹D. M. Edwards, A. C. M. Green, and K. Kubo, cond-mat/9901133 (unpublished).
- ¹⁰A. J. Millis, P. B. Littlewood, and B. I. Shraiman, *Phys. Rev. Lett.* **74**, 5144 (1995).
- ¹¹N. Furukawa, cond-mat/9812066 (unpublished).
- ¹²C. M. Varma, *Phys. Rev. B* **54**, 7328 (1996).
- ¹³A. J. Millis, B. I. Shraiman, and R. Mueller, *Phys. Rev. Lett.* **77**, 175 (1996).
- ¹⁴A. S. Alexandrov and A. M. Bratkovsky, *Phys. Rev. Lett.* **82**, 141 (1999).
- ¹⁵S. Yarlagadda, *Phys. Rev. B* **62**, 14 828 (2000).
- ¹⁶D. Khomskii, cond-mat/0004034 (unpublished).
- ¹⁷A canonical example for the behavior of the second type is the $\text{La}_{0.7}\text{Sr}_{0.3}\text{MnO}_3$ compound, while the most well-studied system of the first group is $\text{La}_{0.67}\text{Ca}_{0.33}\text{MnO}_3$.
- ¹⁸S.-W. Cheong and H. Y. Hwang, in *Colossal Magnetoresistance*, edited by Y. Tokura (Gordon and Breach, New York, 1998).
- ¹⁹L. Sheng, D. Y. Xing, D. N. Sheng, and C. S. Ting, *Phys. Rev. B* **56**, R7053 (1997).
- ²⁰Q. Li *et al.*, cond-mat/9612046 (unpublished).
- ²¹L. Sheng, D. Y. Xing, D. N. Sheng, and C. S. Ting, *Phys. Rev. Lett.* **79**, 1710 (1997).
- ²²H. Y. Hwang, S.-W. Cheong, P. G. Radaelli, M. Marezio, and B. Batlogg, *Phys. Rev. Lett.* **75**, 914 (1995).
- ²³S. Shimomura, N. Wakabayashi, H. Kuwahara, and Y. Tokura, *Phys. Rev. Lett.* **83**, 4389 (1999).
- ²⁴L. Vasiliu-Doloc, S. Rosenkranz, R. Osborn, S. K. Sinha, J. W. Lynn, J. Mesot, O. H. Seeck, G. Preosti, A. J. Fedro, and J. F. Mitchell, *Phys. Rev. Lett.* **83**, 4393 (1999).
- ²⁵P. W. Anderson and H. Hasegawa, *Phys. Rev.* **100**, 675 (1955).
- ²⁶H. Röder, R. R. P. Singh, and J. Zang, *Phys. Rev. B* **56**, 5084 (1997).
- ²⁷M. J. Calderon and L. Brey, *Phys. Rev. B* **58**, 3286 (1998).
- ²⁸S. Yunoki, J. Hu, A. L. Malvezzi, A. Moreo, N. Furukawa, and E. Dagotto, *Phys. Rev. Lett.* **80**, 845 (1998).
- ²⁹A. Chattopadhyay, A. J. Millis, and S. Das Sarma, *Phys. Rev. B* **61**, 10 738 (2000).
- ³⁰L. F. Mattheiss (unpublished).
- ³¹Y. Moritomo, A. Asamitsu, and Y. Tokura, *Phys. Rev. B* **51**, 16 491 (1995).
- ³²D. Das Sarma, N. Shanthi, S. R. Krishnakumar, T. Saitoh, T. Mizokawa, A. Sekiyama, K. Kobayashi, A. Fujimori, E. Weschke, R. Meier, G. Kaindl, Y. Takeda, and M. Takano, *Phys. Rev. B* **53**, 6873 (1996).
- ³³W. E. Pickett and D. J. Singh, *Phys. Rev. B* **53**, 1146 (1996).
- ³⁴The coefficient of 1/3 is introduced so that the Gaussian distribution ρ_g will yield the same second moment $\langle \varepsilon^2 \rangle$ as the actual density of states—see Fig. 4.
- ³⁵I. F. Lyuksyutov and V. Pokrovsky, cond-mat/9808248 (unpublished).
- ³⁶W. Kohn and J. M. Luttinger, *Phys. Rev.* **108**, 590 (1957); J. M. Luttinger and W. Kohn, *ibid.* **109**, 1892 (1958).
- ³⁷A. Urushibara, Y. Morimoto, T. Arima, A. Asamitsu, G. Kido, and Y. Tokura, *Phys. Rev. B* **51**, 14 103 (1995).
- ³⁸J. Inoue and S. Maekawa, *Phys. Rev. Lett.* **74**, 3407 (1995).
- ³⁹V. N. Smolyaninova, X. C. Xie, F. C. Zhang, M. Rajeswari, R. L. Greene, and S. Das Sarma, cond-mat/9903238 (unpublished).
- ⁴⁰P. C. Hohenberg and B. I. Halperin, *Rev. Mod. Phys.* **49**, 435 (1977).